Spanish Journal of Agricultural Research
20 (1), e1102, 9 pages (2022)
eISSN: 2171-9292
https://doi.org/10.5424/sjar/2022201-18631
INIA-CSIC

RESEARCH ARTICLE

OPEN ACCESS

Use of two relative depths of the soil apparent electrical conductivity to define experimental blocks with spatial regression models

Edwin F. Grisales, Aquiles E. Darghan, and Carlos A. Rivera

Universidad Nacional de Colombia, Facultad de Ciencias Agrarias. Bogotá, Colombia

Abstract

Aim of study: Our main objective was to take advantage of the ECa information that the EM38-MK2 sensor records simultaneously at two relative depths for modeling using spatial regression and the subsequent blocking of the conductivity estimate values, incorporating elevation.

Area of study: A 23.1-ha field located in the municipality of Puerto López (Meta, Colombia).

Material and methods: A series of georeferenced data (15438) was collected from the EM38-MK2 sensor, through which the ECa was obtained at two depths, a spatial aggregation was performed using a grid of 40 m × 40 m (167 grid cells), to provide data in Lattice form, the centroid of the cells was determined as the new representative spatial coordinates, to adjust a Spatial Autoregression Model (SAC), and then define the blocks from the predictions of the adjusted model.

Main results: The adjusted model has a comparative purpose with the usual proposals for delimiting management zones separately, so it was convenient to incorporate in the model a 3D weighting matrix relating the two relative depths recorded by the EM38MK2 sensor. By mapping the surface layer with the predictions of the SAC model, two distinguishable blocks were delimited in its ECa and management zone analyst (MZA), which can be suitable for experimentation or agricultural management.

Research highlights: These results can be adopted to define the shape and dimension of the blocks in the context of experimental design so that with adequate blocking, the effect of spatial dependence associated with the physicochemical properties of soils related to ECa can be mitigated or suppressed.

Additional key words: large-scale blocking; precision agriculture; management zone analyst

Abbreviations used: EC (electrical conductivity); ECa (soil apparent electrical conductivity); ECa-075 (ECa at a relative depth of 75 cm); ECa-150 (ECa at a relative depth of 150 cm); EMI (electromagnetic induction); FPI (fuzziness performance index); NCE (normalized classification entropy); MZA (management zone analyst).

Authors' contributions: Conceived and designed the experiments: AED and EFG. All authors participated in the statistical analysis and interpretation of data, drafting and critical revision of the manuscript for important intellectual content.

Citation: Grisales, EF; Darghan, AE; Rivera, CA (2022). Use of two relative depths of the apparent electrical conductivity to define experimental blocks using spatial regression models. Spanish Journal of Agricultural Research, Volume 20, Issue 1, e1102. https://doi.org/10.5424/sjar/2022201-18631

Received: 15 Jul 2021. **Accepted:** 07 Feb 2022.

Funding: The authors received no specific funding for this work

Competing interests: The authors have declared that no competing interests exist.

Data availability statement (DAS): The data that support the findings of this study are openly available at https://drive.google.com/drive/folders/1lX40YNNhZssE8BUNLcSI1DPo8gbmqAb9, reference "Data - Use of the two relative depths of apparent electrical conductivity"

Correspondence should be addressed to Edwin F. Grisales-Camargo: efgrisalesc@unal.edu.co

Introduction

Precision agriculture involves the use of a set of techniques aimed at optimizing the use of agricultural inputs by quantifying the spatial or spatio-temporal variability of agricultural production as well as the variables that define production such as physical properties, soil chemistry, etc. (Chartuni *et al.*, 2007). The values of most soil properties do not have a random pattern of distribution in space. They are spatially correlated with spatial dependence, *i.e* their variables are regional (Yrigoyen, 2003). Although each property could have its own spatial pattern, many of these properties are interrelated. A global handling of them is possible among multivariate patterns or a smaller set of properties could possibly collect the information of the majority, like for example, the soil apparent electrical conductivity (ECa) (Moral *et al.*, 2010). A strategy of precision agricultural management may have, as one of its objectives, the delimitation of areas of common crop management, to give specific management to each area; for example, differentiated site-specific fertilization or irrigation by management zones is based on

the characteristic properties of the soil resulting from each zone. Although this is the usual way of dealing with delimitation, it can also be used to define the shape and size of experimental blocks in the context of experimental design, as this can be convenient in suppressing or eliminating the spatial dependence found in many edaphic properties in the context of standard linear modeling.

ECa has been used to delimit management areas for several years, since it is influenced by a combination of physical properties of the soil that determine its fertility and the crop yield (Millán *et al.*, 2019). Numerous investigations have been conducted with ECa, which report a relationship with different soil properties, among which we can mention: estimation of spatial variability of salinity (Xie *et al.*, 2021), soil water content (El-Naggar *et al.*, 2021), targeted soil sampling (Saey *et al.*, 2009), clay content and cation exchange capacity (Corwin & Lesch, 2005), soil hydraulic properties (Rezaei *et al.*, 2016), and site-specific management zoning (Peralta & Costa, 2013).

This same property has been used to evaluate the content of organisms (not necessarily pathogens) such as earthworms (indicator of soil quality), so that this same property can undoubtedly be used to study the physico-chemical relationships of the soils but also other properties of biological interest, all most certainly related to crop yield (Joschko *et al.*, 2010). Thus, blocking by ECa can be a very convenient strategy in data modeling because instead of involving gradients attributed to one or very few variables, blocking with this property would allow the homogenization of a great variety of physical, chemical and biological properties of soils.

ECa is a depth-weighted, average conductivity measurement for a column of earthen materials to a specific depth (Doolittle & Brevik, 2014). Variations in ECa are produced by changes in the electrical conductivity of earthen materials. ECa will increase with increases in soluble salt, water, clay contents, and temperature (Pedrera *et al.*, 2017; Corwin & Scudiero, 2019). An increasing number of commercially available electromagnetic induction (EMI) sensors are available. EMI sensors commonly used in agriculture and soil investigations include the DUALEM-1, DUALEM-2, DUALEM-21S, and DUALEM-4 meters (Dualem, Inc., Milton, ON, Canada); the EM31, EM34, EM38, EM38-DD, and EM38-MK2 meters (Geonics Ltd., Mississauga, ON, Canada); Veris 3100 and Veris 3150 (Veris Technologies Inc., Salina, KS, USA). These EMI sensors transmit a primary electromagnetic field, which induces electrical currents in the soil. These currents generate a secondary electromagnetic field, which is read by the sensor's receiver. Under conditions known as “operating under low induction numbers”, the secondary field is proportional to the ground current and is used to calculate the “apparent” or “bulk” electrical conductivity (ECa) for the volume of soil profiled (Doolittle & Brevik, 2014).

The EM38-MK2 has two receiver coils spaced at 0.5 m and 1 m from the transmitter coil. The ECa is detected simultaneously at two measuring depths. The sensor provides two measurements of ECa at two relative depths, 0.75 m and 1.50 m, on the mode vertical (Heil & Schmidhalter, 2015). Usually when passing the sensor both ECa measurements are recorded, but it is also usual to model and map the conductivity of one of the modes for the delimitation of the zones. In this research ECa, as a function of relative depth, is modeled by spatial regression for an aggregation of 40 m × 40 m (the minimum that fulfilled the assumptions necessary for modeling). Since the ECa is a function of depth, the measurements from each depth were used to create a spatial weights matrix with all the information from the R^3 space corresponding to the data obtained with the sensor. After spatial aggregation, the centroid of each cell was used to represent the point of aggregation of the values for each cell. The objective of the research was to obtain a single model with all the recorded information and make predictions for each depth and not as it is usually done, that is, taking the data of each depth and adjusting the models marginally (Deakin *et al.*, 2002; Callegary *et al.*, 2007; Medeiros *et al.*, 2018). Finally, applying the fuzzy cluster analysis algorithm, homogeneous conductivity regions were mapped to delimit blocking areas that could be useful in large-scale experimentation (Zhang *et al.*, 2020).

Material and methods

Study area

The study was carried out in a 23.1-ha field, located in the municipality of Puerto López (Meta, Colombia), in the Hato Grande farm, 55 km from Puerto López - Puerto Gaitán, with coordinates 4.2120° N 72.4900° W at an altitude of approximately 212 m.a.s.l. (Fig. 1a). According to the Köppen classification system, it belongs to the tropical rainy savanna climate (Aw). The landscape is mainly composed of alluvial clays, forming surfaces with flat relief and slopes between 1% and 3%. According to the general study of soils and land zoning in the Department of Meta, the taxonomic component is a Typic hapludox association, with characteristics of deep to moderately deep, fine to medium textures, well to moderately drained, strongly to moderately acidic, low fertility, and moderate aluminum toxicity (IGAC, 2005).

Sensor EM38-MK2 and field measurement

Data collection in the ECa field was carried out with calibrated EM38-MK2 equipment *in situ* under the GEONICS (2012) methodology. The ECa data were taken

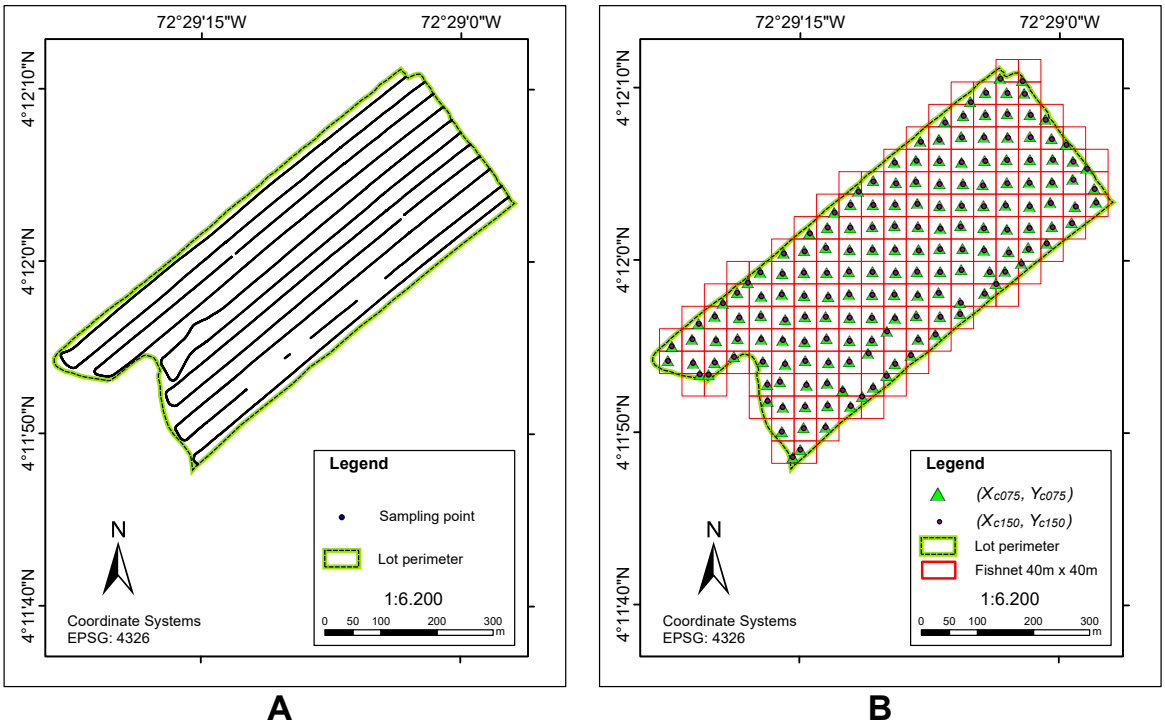

Figure 1. a) Location of the study area; b) representation of the centroids for each layer. Triangle (top layer) and point (bottom layer).

with a mean temperature of 25.2 ºC, which were adjusted following the methodology of Corwin & Lesch (2005) with an f_t = 0.9953, where f_t is a temperature conversion factor. Dense sampling was performed in passes approximately parallel to the study area, connecting the sensor to a Hemisphere GPS XF101 DGPS unit (Juniper Systems, Inc., Logan, UT, USA) that recorded the location of each measurement in World Geodetic System 1984 (WGS84) along with elevation. The sensor provided data with an effective depth of 1.50 m (ECa-150) and 0.75 m (ECa-075). In our study the sensor reported 15438 georeferenced points in the area at an average distance between passes of 30 m at an average tractor speed of 3.0 km/h, for an approximate sampling intensity of 668 points per hectare.

Spatial data aggregation and representative coordinate

A 40 m × 40 m square network was generated with the Create Fishnet tool of ArcGIS 10.5.1 (ESRI, 2017) to estimate the mean of the sampled ECa-075 and ECa-150 points that spatially intercepted each of the cells in the network. The geometric centroid (x_c, y_c) was used as the representative coordinate for each cell that was different for each cell of the network between different layers, due to the weight that the ECa itself exerted on each coordinate (Deakin *et al.*, 2002). The numerical values that accompany the pair (x_c, y_c) as subscripts refer to each of the depths used.

For each of the cells of the network, we obtained the representative coordinate for each relative depth of ECa-075 and ECa-150 (Fig. 1b).

Spatial regression models

Prior to modeling with spatial regression (spatial data for areas), the assumptions for the application of various geostatistical methods were explored, and it became evident that there was a very low possibility of using these methods that usually require strong assumptions for their use, and although some people ignore them because their interest seems to be more in the visualization that is obtained, their use without checking the assumptions certainly invalidates the results (Webster & Oliver, 2007; Arbia, 2014; Christensen, 2018). Spatial regression models are commonly used to analyze spatial processes in a network (Li *et al.*, 2007). The spatial regression model initially used according to the taxonomy of Elhorst (2014) was finally the spatial autocorrelation model (SAC) (Santos *et al.*, 2018; Rodríguez *et al.*, 2019) that is written as:

$$Y = \lambda WY + \alpha\iota_m + X\beta + u$$
$$u = \rho Wu + \varepsilon \quad (1)$$

where Y epresents the response variable associated with the ECa added in each cell (with vector length equal to $m=2n$, where n presents each of the measurements in one of the layers or depths); λ is known as the autoregressive spatial coefficient; W represents the matrix of spatial

weights ($2n \times 2n$); α represents the intercept; ι_m is a unit vector of length $2n$; X is the vector corresponding to the terrain elevation adjusted by the relative depth reached by the sensor of the ECa associated with the geometric centroid that in the case of this research represents the depths of 0.75 m (d_1) and 1.50 m (d_2) ($X=Z-d$, with $d_m=[d_1,d_2]'\otimes \iota_n$, where $\otimes$ is the Kronecker product and Z representing the elevation) (Zhang & Ding, 2013); β is the scalar associated with the terrain elevation adjusted; u is the vector of residuals expected to have some spatial dependency structure that is decomposed in the form expressed in the lower part of Eq. (1), where ρ is the spatial autocorrelation coefficient, and ε are the residuals that are expected to be normal and independent with identical distribution, with mean 0 and variance σ^2.

The term WY denotes the endogenous effect associated with the spatial lag of the response variable caused by the matrix of spatial weights generated from the distances between the centroids of the polygons used of the intra-layers and inter-layers. This is a non-negative matrix normalized from the dimension $m \times m$. Usually, the W matrix is built for each layer separately; and in fact, it is modeled in the same way. However, in this case the *mat2listw* function from the R *spdep* library (Bivand & Wong, 2018) was used to configure a matrix of weights involving distances within and between layers. For this case, the evaluated weight matrix was determined with a function of the inverse of the distance (Longley *et al.*, 2015). For the model finally selected, the assumptions of independence of the residuals (ε), spatial dependence of the residuals (u), and distributional behavior of the residuals were reviewed. The review used the Monte Carlo test of the *Moran index* with the *moran.mc* function and 5,000 simulations, programmed in the spdep library of R (Bivand & Wong, 2018), and the skewness normality test (Shapiro *et al.*, 1968) of the *normtest* library of R (Gavrilov & Pusev, 2014). It is important to note that, although results of the aggregation of 40 m × 40 m are presented, the modeling started from an aggregation of 5 m × 5 m to 150 m × 150 m at an arithmetic ratio of 5 m, with the aggregation of 40 m × 40 m as the minimum that met the assumptions for the model fit. Finally, for this aggregation, the vector of ECa (Y) was of longitude 334 and the dimension of W was 334×334.

Finally, when fitting model (1), the residuals u turned out to be independent ($u=\varepsilon$), so that finally the spatial model of the error given only by the upper part of (1) was fitted:

$$Y = \lambda WY + \alpha\iota_m + X\beta + \varepsilon\,. \qquad (2)$$

After the model was fitted, model predictions were made and subsequently separated for each depth layer so that the delineation of the blocking areas of the approach could be contrasted by fitting one model per layer with our approach to predictions with a single two-layer model using the K-means fuzzy cluster analysis algorithm in R software (Fridgen *et al.*, 2004; Meyer *et al.*, 2021). To determine the optimal number of zones, we estimated the indices of Xie-Beni (Xie & Beni, 1991), Fukuyama-Sugeno (Fukuyama, 1989), the coefficients of entropy of classification (also known as the *Fuzziness Performance Index* - FPI and *Normalized Classification Entropy* - NCE), which were calculated using the *fclusterIndex* function of the R *e1071* library (Meyer *et al.*, 2021). Finally, the blocking zones were delimited for large-scale experimentation. This was done only for the upper layer because most of the crops have a root system that reaches only up to a depth of 75 cm (Fan *et al.*, 2016; Zhang *et al.*, 2017).

Results

In Table 1, a descriptive statistical analysis of the original data, the temperature adjusted data and the spatial aggregation with a size of 40 × 40 for both ECa-075 and ECa-150 was performed. In addition, an exploratory

Table 1. Descriptive statistics of apparent soil electrical conductivity (ECa)

	Original data		Data adjusted for temperature		Data with a spatial aggregation of 40 m × 40 m		Values estimated by the spatial model
	ECa-075	ECa-150	ECa-075	ECa-150	ECa-075	ECa-150	ECa-075
Minimum	6.28	15.82	6.25	15.74	6.80	16.92	8.48
Maximum	15.74	21.86	15.66	21.76	13.20	20.66	13.65
Mean	10.10	18.59	10.05	18.50	9.96	18.51	11.69
Median	9.85	18.56	9.80	18.48	9.85	18.53	11.68
Standard deviation	1.46	0.85	1.45	0.85	1.32	0.69	0.99
Asymmetry	0.51	0.10	0.51	0.10	0.28	0.29	-0.54
Kurtosis	2.92	3.13	2.92	3.13	2.54	3.17	3.11
Coefficient of variation	14.47	4.57	14.47	4.57	13.29	3.72	8.47
No. of total data	15438	15438	15438	15438	167	167	167

Table 2. Estimated parameters in model (a: asymptotic)

Parameter	Estimate	Standard error	Test Z value	*p* value
Intercept	5.068	3.836	1.321	0.186
Elevation	0.045	0.019	2.390	0.017
Lambda (λ)	-0.870	0.022a	-38.868	2.2E-16

analysis of the ECa-075 data was performed on the values estimated by the spatial model.

Table 2 presents the results of the fitted model. The results show statistical evidence against the null hypothesis associated with the null effect of the implied term (intercept and auto-regressive coefficient). Table 3, shows the values of the estimated variance of the residuals, the Akaike's information criterion and the results of the spatial autocorrelation test using Moran's index; the latter being of relevant importance in the selection of the final spatial regression model, as well as the results of the residual normality test. These results show normality and spatial independence of the residuals.

The adjusted model has a comparative purpose with the usual proposals of delimiting regions separately, thus, it is convenient in this case to evaluate the model with a 3D weight matrix with the models that use 2D weight matrices, so in both cases the entire data set was used. Cross-validation is more restrictive in spatial data because of the assumption of non-exchangeability that must be met. Being spatial data, the Bootstrap or Jackknife methods for cross-validation require a specialized treatment in these cases and applying them here diverts the interest of the research in comparing two modalities of delimitation of regions.

After implementing the general model in Eq. (2), the ECa was estimated and then the data points corresponding to a depth of 75 cm were selected. With this portion of the data, the large-scale experimental blocking zones were delimited using K-means fuzzy cluster analysis, generating 2, 3, 4 and 5 (I2CM, I3CM, I4CM and I5CM). Once the zones were delimited, the optimal number of zones was determined using the Xie-Beni, Fukuyama-Sugeno, FPI and NCE indices. Table 4 shows the results of the indices to illustrate the mechanism for choosing the number of zones (lowest index value) proposed by Córdoba *et al.* (2014). For all the indices determined, the optimum number of zones was two, except for Fukuyama-Sugeno.

Table 5 shows the areas (in ha) related to each management zone, estimated from the methodology used. In Fig. 2, the delimitation of management zone analyst (MZA) is represented in a smoothed form using the cubic convolution technique as resampling for information visualization in ArcGIS 10.5.1 software.

For the characterization of the zones, univariate descriptive statistics of ECa and elevation were obtained for each zone in the upper layer (Table 5). In Fig. 3, a bivariate analysis of ECa and elevation for both zones can be seen, generated with the help of RStudio by calling the *ggpairs* function of the *ggplot2* library.

Clearly the ECa is discriminated in the two regions selected for large-scale experimental blocking, but this is not the case for the elevation variable, so that zone 1 is typified as high ECa and zone 2 as low ECa, This defines the two levels of the blocking factor for the subsequent randomization of the treatments in these zones, either considering the blocks as the entire defined region or selecting subplots within each block to generate replicates that allow the evaluation of more complex design models in complete, incomplete or generalized blocks, as well as a balanced or unbalanced structure.

Discussion

Electrical conductivity modeling is usually done through geostatistical procedures due to the nature of the data. However, spatial regression is another spatial data modeling technique that can yield results similar to geostatistics but with greater simplicity in fulfilling assumptions for the adjustment of the models. Only it will depend on the spatial aggregation used with respect to the creation of the grids on the scale used. For the current case, a series of models with different aggregation sizes were adjusted. But finally, we selected the one with the smallest cell size (40 m × 40 m) that met the required assumptions of the modeling procedure. This turned out to be a routine task, easy to program in both ArcGIS and RStudio. Compared to the application of the Kriging method or the semivariogram model, this was simpler due to the assumptions necessary for the application of geostatistical methods.

When using ECa sensors, it is possible to obtain measurements of this variable at two depths for the same geographic coordinate. The most usual is to model each measurement separately (Sudduth *et al.*, 2003; 2013) or by obtaining the normalized difference of the two depths to generate a single measurement (Martinez *et al.*, 2009).

Table 3. Statistics of the residuals and the spatial autocorrelation model, Monte-Carlo of Moran index simulation and normality test (skewness normality test) for residual.

Residual variance (ML)	AIC	I moran (residual)		Normality test (residual)	
		statistic	*p*-value	T	*p*-value
4.690	1643.79	-0.206	0.999	-0.114	0.375

ML = Maximum Likelihood; AIC = Akaike information criterion.

Table 4. Determination of the zones or blocks by means of the indices for clustering

Index	I2CM	I3CM	I4CM	I5CM
Xie-Beni	5.50×10^{-4}	8.01×10^{-4}	8.20×10^{-4}	7.90×10^{-4}
Fukuyama-Sugeno	-1.58×10^{2}	-1.01×10^{2}	-1.52×10^{2}	-1.64×10^{2}
FPI	1.041	1.049	1.057	1.063
NCE	6.82×10^{-2}	7.91×10^{-2}	8.93×10^{-2}	10.00×10^{-2}

FPI = fuzziness performance index; NCE = normalized classification entropy.

Table 5. Area (in hectares) by management zones

	Zone 1	Zone 2	Zone 3	Zone 4	Zone 5
I2CM	11.1	12.0	—	—	—
I3CM	10.1	11.3	1.7	—	—
I4CM	7.0	7.5	1.7	6.9	—
I5CM	6.6	6.8	0.9	5.3	3.5

However, it is unusual to incorporate the two depths into a single model using a matrix of 3D spatial weights between the points aggregated to the centroid of each grid cell used. This work allowed us to delineate the two blocking regions using the top layer ECa estimates in the visualization but using all the data in the spatial model building process. The data provided evidence against the null effect for both the depth-adjusted elevation variable and the autoregressive coefficient associated with ECa. The adjusted elevation refers to the fact that the 75 cm depth was added to the elevation value as well as the 150 cm depth, as appropriate.

The modeling of each measure of electrical conductivity apparent by depth is somewhat usual, as shown in Badewa *et al.* (2018) and in Robinet *et al.* (2018). Although it was possible to do the same as these authors and many others, this time it was possible to try a different alternative to take advantage of the correlation that usually exists between conductivities of each depth but only to map the upper layer where the agronomic interest is usually (Medeiros *et al.*, 2018).

Another important aspect in the construction of appropriate blocks that respond to the set of physical, chemical and biological properties of the soil is the effect it can have on statistical modeling by analysis of variance in the standard linear model, where the assumption of independence of residuals is often required. Successful blocking can reduce or even suppress the spatial dependence of residuals in the model, which can be evidenced either by

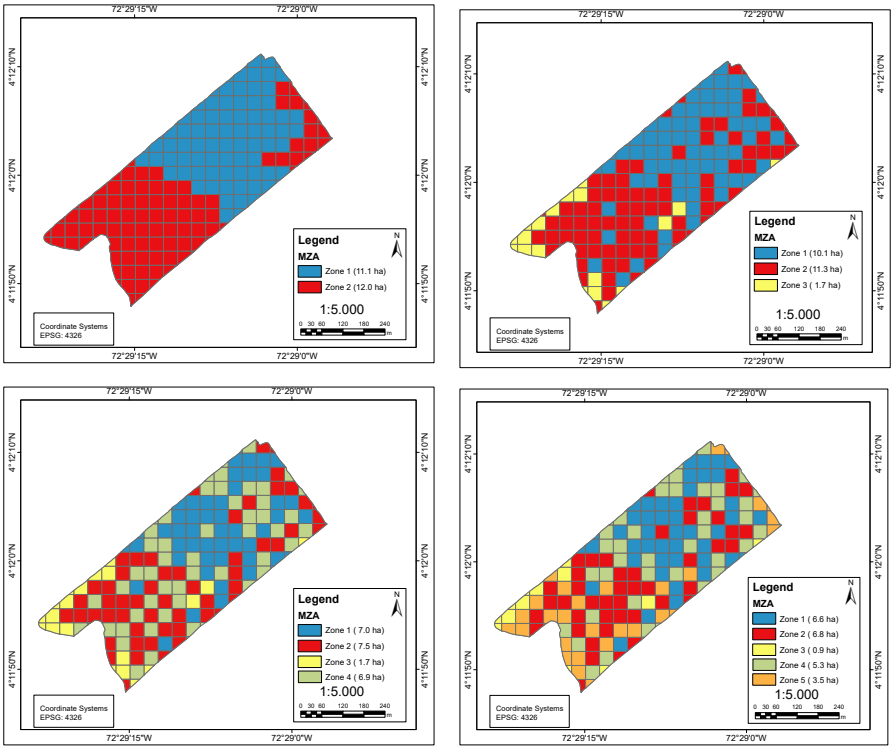

Figure 2. Management zone analyst (MZA) delimitation using experimental blocking, for 2 zones, 3 zones, 4 zones and 5 zones.

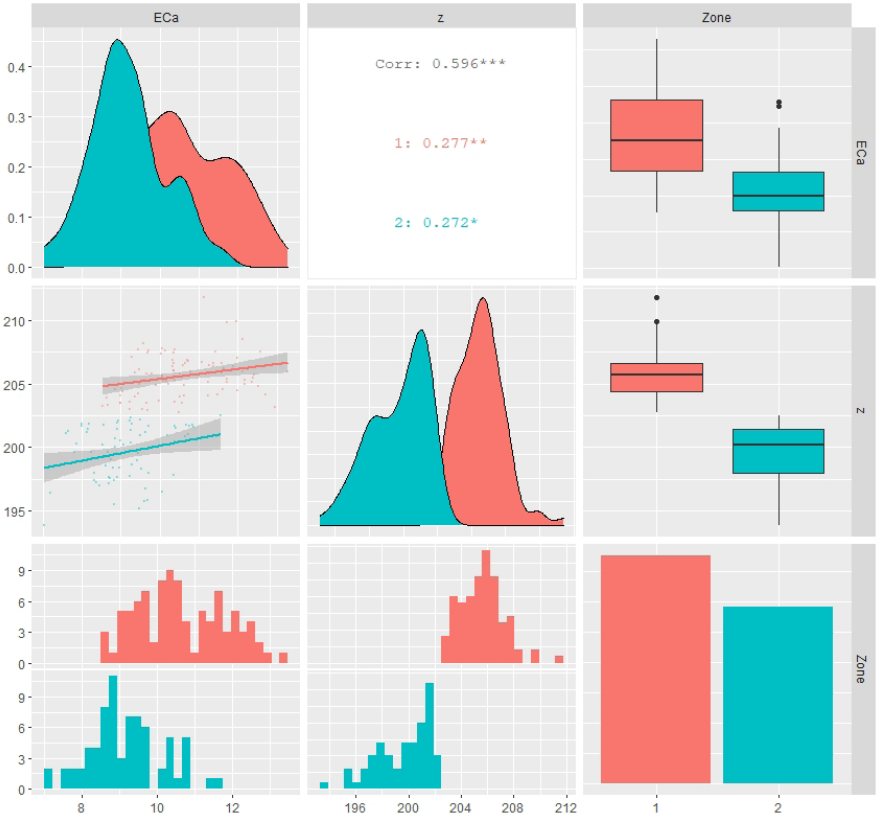

Figure 3. Descriptive statistics by zones.

the efficiency of blocking in the comparison of the model with and without blocks using the Moran index as a measure of spatial dependence. It should be remembered that the use of the F distribution in the analysis of variance is questionable in the presence of spatial dependence (Gotway & Cressie, 1990), so its suppression by an adequate blocking is convenient in the context of experimental design and standard linear modeling.

In conclusion, the incorporation of both proximal sensor ECa measures into the spatial regression modeling process proved to be a reproducible strategy for generating regions for large-scale experimental blockage. The use of ECa as a measure related to a large number of physical, chemical and biological variables soil allowed the generation of blocking levels that consider the elevation of the ground in addition to the information of ECa at two depths. Spatial modeling with spatial regression incorporating 3D weight matrices yielded different results in mapping electrical conductivity to generate blocking regions for large-scale experimentation in these cases when building a single model for each depth of conductivity, thus taking into account the simultaneous information can be crucial in the delimitation of the blocking zones. This has the advantage of taking into account in the modeling process the correlation that was evidenced between both conductivity measurements. Spatial regression modeling proved to be a flexible alternative in spatial modeling, especially when assumptions for geostatistical analysis are restrictive or not easily found. The use of single layer data and thus a spatial regression model for this same layer could imply a smaller amount of data which, as in our case, did not allow for the fitting of a model and thus the construction of the blocking zones. However, the information related to the two depths gave us a larger number of data, which allowed the fitting of the model and thus the generation of the blocking zones.

References

Arbia G, 2014. A primer for spatial econometrics with applications in R. Palgrave Macmillan, UK. https://doi.org/10.1057/9781137317940

Badewa E, Unc A, Cheema M, Kavanagh V, Galagedara L, 2018. Soil moisture mapping using multi-frequency and multi-coil electromagnetic induction sensors on managed podzols. Agronomy 8(10): 224-239. https://doi.org/10.3390/agronomy8100224

Bivand R, Wong D, 2018. Comparing implementations of global and local indicators of spatial association. Test 27(3): 716-748. https://doi.org/10.1007/s11749-018-0599-x

Callegary J, Ferré T, Groom R, 2007. Vertical spatial sensitivity and exploration depth of low-induction-number electromagnetic-induction instruments. Vadose Zone J 6(1): 158-167. https://doi.org/10.2136/vzj2006.0120

Chartuni E, De Assis F, Marcal D, Ruz E, 2007. Precision agriculture: new tools to improve technology management in agricultural enterprises. Com Mag 16: 24-31.

Christensen R, 2018. Analysis of variance, design, and regression: Linear modeling for unbalanced data. CRC Press, USA. https://doi.org/10.1201/9781315370095

Córdoba M, Bruno C, Aguate F, Tablada M, Balzarini M, 2014. Análisis de la variabilidad espacial en lotes agrícolas. Manual de buenas prácticas agrícolas. Eudecor, Argentina.

Corwin D, Lesch S, 2005. Apparent soil electrical conductivity measurements in agriculture. Comput Electron Agr 46(1-3): 11-43. https://doi.org/10.1016/j.compag.2004.10.005

Corwin D, Scudiero E, 2019. Mapping soil spatial variability with apparent soil electrical conductivity (ECa) directed soil sampling. Soil Sci Soc Am J 83(1): 3-4. https://doi.org/10.2136/sssaj2018.06.0228

Deakin R, Bird S, Grenfell R, 2002. The centroid? Where would you like it to be be? Cartography 31 (2): 153-167. https://doi.org/10.1080/00690805.2002.9714213

Doolittle J, Brevik E, 2014. The use of electromagnetic induction techniques in soils studies. Geoderma (223): 33-45. https://doi.org/10.1016/j.geoderma.2014.01.027

Elhorst J, 2014. Spatial econometrics from cross-sectional data to spatial panels. Springer, USA. https://doi.org/10.1007/978-3-642-40340-8

El-Naggar A, Hedley C, Roudier P, Horne D, Clothier B, 2021. Imaging the electrical conductivity of the soil profile and its relationships to soil water patterns and drainage characteristics. Precis Agr 22: 1045-1066. https://doi.org/10.1007/s11119-020-09763-x

ESRI, 2017. ArcGIS desktop Release 10.5.1. Env Syst Res Inst (844): 845. Redlands, CA, USA.

Fan J, McConkey B, Wang H, Janzen H, 2016. Root distribution by depth for temperate agricultural crops. Field Crops Res 189: 68-74. https://doi.org/10.1016/j.fcr.2016.02.013

Fridgen J, Kitchen N, Sudduth K, Drummond S, Wiebold W, Fraisse C, 2004. Management Zone Analyst (MZA) software for subfield management zone delineation. Agron J 96(1): 100-108. https://doi.org/10.2134/agronj2004.1000

Fukuyama Y, 1989. A new method of choosing the number of clusters for the fuzzy c-mean method. Proc Fuzzy Syst Symp 5: 247-250.

Gavrilov I, Pusev R, 2014. Normtest: Tests for Normality. R package CRAN 1.1: 1-14.

GEONICS, 2012. Ground conductivity meter operating manual EM38MK2. Geonics Ltd. Lead Electr, p: 57. Ontario, Canada.

Gotway C, Cressie N, 1990. A spatial analysis of variance applied to soil-water infiltration. Water Resour Res 26(11): 2695-2703. https://doi.org/10.1029/WR026i011p02695

Heil K, Schmidhalter U, 2015. Comparison of the EM38 and EM38-MK2 electromagnetic induction-based sensors for spatial soil analysis at field scale. Comput Electron Agr 110: 267-280. https://doi.org/10.1016/j.compag.2014.11.014

IGAC, 2005. Estudio general de suelos y zonificación de tierras del Departamento de Meta. Inst Geog Agus Coda, Bogotá, Colombia. 159 pp.

Joschko M, Gebbers R, Barkusky D, Timmer J, 2010. The apparent electrical conductivity as a surrogate variable for predicting earthworm abundances in tilled soils. J Plant Nut Soil Sci 173(4): 584-590. https://doi.org/10.1002/jpln.200800071

Li H, Calder C, Cressie N, 2007. Beyond Moran's I: testing for spatial dependence based on the spatial autoregressive model. Geog Analy 39(4): 357-375. https://doi.org/10.1111/j.1538-4632.2007.00708.x

Longley P, Goodchild M, Maguire D, Rhind D, 2015. Geographic information science and systems. Wiley, USA.

Martinez G, Vanderlinden K, Ordóñez R, Muriel J, 2009. Can apparent electrical conductivity improve the spatial characterization of soil organic carbon? Vad Zone J 8(3): 586-593. https://doi.org/10.2136/vzj2008.0123

Medeiros W, Valente D, Queiroz D, Pinto F, Assis I, 2018. Apparent soil electrical conductivity in two different soil types1. Rev Ciên Agron 49: 43-52. https://doi.org/10.5935/1806-6690.20180005

Meyer D, Dimitriadou E, Hornik K, Weingessel A, Leisch F, Chang C, Lin C, 2021. e1071: Misc Functions of the Department of Statistics, Probability Theory Group. R package CRAN (1.7): 1-66.

Millán S, Moral F, Prieto M, Pérez-Rodriguez J, Campillo C, 2019. Mapping soil properties and delineating management zones based on electrical conductivity in a hedgerow olive grove. T ASABE 62(3): 749-760. https://doi.org/10.13031/trans.13149

Moral F, Terrón J, Da Silva J, 2010. Delineation of management zones using mobile measurements of soil apparent electrical conductivity and multivariate geostatistical techniques. Soil Till Res 106(2): 335-343. https://doi.org/10.1016/j.still.2009.12.002

Pedrera A, Pachepsky Y, Taguas E, Martos S, Giráldez J, Vanderlinden K, 2017. Concurrent temporal stability of the apparent electrical conductivity and soil water content. J Hydr 544: 319-326. https://doi.org/10.1016/j.jhydrol.2016.10.017

Peralta N, Costa J, 2013. Delineation of management zones with soil apparent electrical conductivity to improve nutrient management. Comput Electron Agr 99: 218-226. https://doi.org/10.1016/j.compag.2013.09.014

Rezaei M, Saey T, Seuntjens P, Joris I, Boënne W, Van Meirvenne M, Cornelis W, 2016. Predicting saturated hydraulic conductivity in a sandy grassland using

proximally sensed apparent electrical conductivity. J Appl Geoph 126: 35-41. https://doi.org/10.1016/j.jappgeo.2016.01.010

Robinet J, von Hebel C, Govers G, van der Kruk J, Minella J, Schlesner A, *et al.*, 2018. Spatial variability of soil water content and soil electrical conductivity across scales derived from electromagnetic induction and time domain reflectometry. Geoderma 314: 160-174. https://doi.org/10.1016/j.geoderma.2017.10.045

Rodríguez H, Darghan A, Henao M, 2019. Spatial regression modeling of soils with high cadmium content in a cocoa producing area of Central Colombia. Geoderma 16: 214-226. https://doi.org/10.1016/j.geodrs.2019.e00214

Santos P, Roa H, Contreras A, Parra J, 2018. Modelado espacial del carbono orgánico del suelo y su relación con otras propiedades químicas en el cultivo de arroz del distrito de riego del Norte de Santander Colombiano. Gest Amb 21(2): 252-262. https://doi.org/10.15446/ga.v21n2.73004

Saey T, Meirvenne M, Vermeersch H, Ameloot N, Cockx L, 2009. A pedotransfer function to evaluate the soil profile textural heterogeneity using proximally sensed apparent electrical conductivity. Geoderma 150: 389-395. https://doi.org/10.1016/j.geoderma.2009.02.024

Shapiro S, Wilk M, Chen H, 1968. A comparative study of various tests for normality. J Am Stat Assoc 63(324): 1343-1372. https://doi.org/10.1080/01621459.1968.10480932

Sudduth K, Kitchen N, Bollero G, Bullock D, Wiebold W, 2003. Comparison of electromagnetic induction and direct sensing of soil electrical conductivity. Agron J 95(3): 472-482. https://doi.org/10.2134/agronj2003.4720

Sudduth K, Myers D, Kitchen N, Drummond S, 2013. Modeling soil electrical conductivity-depth relationships with data from proximal and penetrating ECa sensors. Geoderma 199: 12-21. https://doi.org/10.1016/j.geoderma.2012.10.006

Webster R, Oliver M, 2007. Geostatistics for environmental scientists. Wiley, UK. https://doi.org/10.1002/9780470517277

Xie X, Beni G, 1991. A validity measure for fuzzy clustering: IEEE Trans Pat Anal Mach Intel 13(8): 1-7. https://doi.org/10.1109/34.85677

Xie W, Yang J, Yao R, Wang X, 2021. Spatial and temporal variability of soil salinity in the Yangtze River estuary using electromagnetic induction. Rem Sens 13(10): 1-16. https://doi.org/10.3390/rs13101875

Yrigoyen C, 2003. Econometría espacial aplicada a la predicción-extrapolación de datos microterritoriales. Dirección General de Economía y Planificación. Com Mad 132: 79-94.

Zhang H, Ding F, 2013. On the Kronecker products and their applications. J Appl Math 13: 1-8. https://doi.org/10.1155/2013/296185

Zhang Y, Han K, Jung K, Cho H, Seo M, Sonn Y, 2017. Study on the standards of proper effective rooting depth for upland crops. Kor J Soil Sci Fert 50: 21-30. https://doi.org/10.7745/KJSSF.2017.50.1.021

Zhang T, Gaffrey M, Monroe M, Thomas D, Weitz K, Piehowski P, *et al.*, 2020. Block design with common reference samples enables robust large-scale label-free quantitative proteome profiling. J Proteom Res 19(7): 2863-2872. https://doi.org/10.1021/acs.jproteome.0c00310